Available online at www.sciencedirect.com
SCIENCE DIRECT®
PHYSICS LETTERS B
Physics Letters B 578 (2004) 16–22
www.elsevier.com/locate/physletb

Measurement of branching ratios for η_c hadronic decays

BES Collaboration

J.Z. Bai [a], Y. Ban [j], J.G. Bian [a], X. Cai [a], J.F. Chang [a], H.F. Chen [p], H.S. Chen [a], H.X. Chen [c], Jie Chen [i], J.C. Chen [a], Y.B. Chen [a], S.P. Chi [a], Y.P. Chu [a], X.Z. Cui [a], H.L. Dai [a], Y.S. Dai [r], Y.M. Dai [g], L.Y. Dong [a], S.X. Du [q], Z.Z. Du [a], J. Fang [a], S.S. Fang [a], C.D. Fu [a], H.Y. Fu [a], L.P. Fu [f], C.S. Gao [a], M.L. Gao [a], Y.N. Gao [n], M.Y. Gong [a], W.X. Gong [a], S.D. Gu [a], Y.N. Guo [a], Y.Q. Guo [a], Z.J. Guo [o], S.W. Han [a], F.A. Harris [o], J. He [a], K.L. He [a], M. He [k], X. He [a], Y.K. Heng [a], H.M. Hu [a], T. Hu [a], G.S. Huang [a], L. Huang [f], X.P. Huang [a], X.B. Ji [a], Q.Y. Jia [j], C.H. Jiang [a], X.S. Jiang [a], D.P. Jin [a], S. Jin [a], Y. Jin [a], Z.J. Ke [a], Y.F. Lai [a], F. Li [a], G. Li [a], H.H. Li [e], J. Li [a], J.C. Li [a], K. Li [f], Q.J. Li [a], R.B. Li [a], R.Y. Li [a], W. Li [a], W.G. Li [a], X.Q. Li [i], X.S. Li [n], Y.F. Liang [m], H.B. Liao [e], C.X. Liu [a], Fang Liu [p], F. Liu [e], H.M. Liu [a], J.B. Liu [a], J.P. Liu [q], R.G. Liu [a], Y. Liu [a], Z.A. Liu [a], Z.X. Liu [a], G.R. Lu [d], F. Lu [a], H.J. Lu [p], J.G. Lu [a], C.L. Luo [h], X.L. Luo [a], E.C. Ma [a], F.C. Ma [g], J.M. Ma [a], L.L. Ma [k], X.Y. Ma [a], Z.P. Mao [a], X.C. Meng [a], X.H. Mo [a], J. Nie [a], Z.D. Nie [a], S.L. Olsen [o], H.P. Peng [p], N.D. Qi [a], C.D. Qian [l], J.F. Qiu [a], G. Rong [a], D.L. Shen [a], H. Shen [a], X.Y. Shen [a], H.Y. Sheng [a], F. Shi [a], L.W. Song [a], H.S. Sun [a], S.S. Sun [p], Y.Z. Sun [a], Z.J. Sun [a], S.Q. Tang [a], X. Tang [a], D. Tian [a], Y.R. Tian [n], G.L. Tong [a], G.S. Varner [o], J.Z. Wang [a], L. Wang [a], L.S. Wang [a], M. Wang [a], Meng Wang [a], P. Wang [a], P.L. Wang [a], W.F. Wang [a], Y.F. Wang [a], Zhe Wang [a], Z. Wang [a], Zheng Wang [a], Z.Y. Wang [b], C.L. Wei [a], N. Wu [a], X.M. Xia [a], X.X. Xie [a], G.F. Xu [a], Y. Xu [a], S.T. Xue [a], M.L. Yan [p], W.B. Yan [a], F. Yang [i], G.A. Yang [a], H.X. Yang [n], J. Yang [p], S.D. Yang [a], Y.X. Yang [c], M.H. Ye [b], Y.X. Ye [p], J. Ying [j], C.S. Yu [a], G.W. Yu [a], C.Z. Yuan [a], J.M. Yuan [a], Y. Yuan [a], Q. Yue [a], S.L. Zang [a], Y. Zeng [f], B.X. Zhang [a], B.Y. Zhang [a], C.C. Zhang [a], D.H. Zhang [a], H.Y. Zhang [a], J. Zhang [a], J.M. Zhang [d], J.W. Zhang [a], L.S. Zhang [a], Q.J. Zhang [a], S.Q. Zhang [a], X.Y. Zhang [k], Yiyun Zhang [m], Y.J. Zhang [j], Y.Y. Zhang [a], Z.P. Zhang [p], D.X. Zhao [a], Jiawei Zhao [p], J.B. Zhao [a], J.W. Zhao [a], P.P. Zhao [a], W.R. Zhao [a], Y.B. Zhao [a], Z.G. Zhao [a,1], J.P. Zheng [a], L.S. Zheng [a], Z.P. Zheng [a], X.C. Zhong [a], B.Q. Zhou [a], G.M. Zhou [a], L. Zhou [a], N.F. Zhou [a], K.J. Zhu [a], Q.M. Zhu [a], Yingchun Zhu [a], Y.C. Zhu [a], Y.S. Zhu [a], Z.A. Zhu [a], B.A. Zhuang [a], B.S. Zou [a]

[a] *Institute of High Energy Physics, Beijing 100039, People's Republic of China*

doi:10.1016/j.physletb.2003.10.042

[b] *China Center of Advanced Science and Technology, Beijing 100080, People's Republic of China*
[c] *Guangxi Normal University, Guilin 541004, People's Republic of China*
[d] *Henan Normal University, Xinxiang 453002, People's Republic of China*
[e] *Huazhong Normal University, Wuhan 430079, People's Republic of China*
[f] *Hunan University, Changsha 410082, People's Republic of China*
[g] *Liaoning University, Shenyang 110036, People's Republic of China*
[h] *Nanjing Normal University, Nanjing 210097, People's Republic of China*
[i] *Nankai University, Tianjin 300071, People's Republic of China*
[j] *Peking University, Beijing 100871, People's Republic of China*
[k] *Shandong University, Jinan 250100, People's Republic of China*
[l] *Shanghai Jiaotong University, Shanghai 200030, People's Republic of China*
[m] *Sichuan University, Chengdu 610064, People's Republic of China*
[n] *Tsinghua University, Beijing 100084, People's Republic of China*
[o] *University of Hawaii, Honolulu, HI 96822, USA*
[p] *University of Science and Technology of China, Hefei 230026, People's Republic of China*
[q] *Wuhan University, Wuhan 430072, People's Republic of China*
[r] *Zhejiang University, Hangzhou 310028, People's Republic of China*

Received 2 September 2003; accepted 13 October 2003

Editor: M. Doser

Abstract

In a sample of 58 million J/ψ events collected with the BES II detector, the process $J/\psi \to \gamma\eta_c$ is observed in five decay channels: $\eta_c \to K^+K^-\pi^+\pi^-$, $\pi^+\pi^-\pi^+\pi^-$, $K^\pm K_S^0\pi^\mp$ (with $K_S^0 \to \pi^+\pi^-$), $\phi\phi$ (with $\phi \to K^+K^-$) and $p\bar{p}$. From these signals, we determine

$$Br(J/\psi \to \gamma\eta_c)Br(\eta_c \to K^+K^-\pi^+\pi^-) = (1.5 \pm 0.2 \pm 0.2) \times 10^{-4},$$

$$Br(J/\psi \to \gamma\eta_c)Br(\eta_c \to \pi^+\pi^-\pi^+\pi^-) = (1.3 \pm 0.2 \pm 0.4) \times 10^{-4},$$

$$Br(J/\psi \to \gamma\eta_c)Br(\eta_c \to K^\pm K_S^0\pi^\mp) = (2.2 \pm 0.3 \pm 0.5) \times 10^{-4},$$

$$Br(J/\psi \to \gamma\eta_c)Br(\eta_c \to \phi\phi) = (3.3 \pm 0.6 \pm 0.6) \times 10^{-5},$$

$$Br(J/\psi \to \gamma\eta_c)Br(\eta_c \to p\bar{p}) = (1.9 \pm 0.3 \pm 0.3) \times 10^{-5}.$$

PACS: 13.25.Gv; 14.40.Gx; 13.40.Hq

Hadronic decays of the η_c have been studied by Mark III [1,2], DM2 [3], and other experiments [4–7]. However, the branching fractions of the η_c still have very large errors in the Particle Data Group (PDG) compilation [8]. More recently the branching fractions for $B \to \eta_c K$ decays and $B \to \eta_c K^*$ have been measured by the Belle [9,10] experiment, and their measured branching fraction for $\eta_c \to \phi\phi$ is smaller than the PDG value [8].

In a previous Letter [11], based on 58 million J/ψ events collected in the Beijing Spectrometer (BES II) detector at the Beijing Electron–Positron Collider, we measured the η_c mass and width using the processes $J/\psi \to \gamma\eta_c$, $\eta_c \to K^+K^-\pi^+\pi^-$, $\pi^+\pi^-\pi^+\pi^-$, $K^\pm K_S^0\pi^\mp$ (with $K_S^0 \to \pi^+\pi^-$), $\phi\phi$ (with $\phi \to K^+K^-$) and $p\bar{p}$, and obtained $m_{\eta_c} = 2977.5 \pm 1.0(\text{stat}) \pm 1.2(\text{sys})$ MeV and $\Gamma_{\eta_c} = 17.0 \pm$

E-mail address: dongly@mail.ihep.ac.cn (L.Y. Dong).
[1] Visiting professor to University of Michigan, Ann Arbor, MI 48109, USA

3.7(stat) $\pm$ 7.4(sys) MeV. In this Letter, we report measurements of the branching ratios for the same processes.

BES is a conventional solenoidal magnet detector that is described in detail in Ref. [12]; BESII is the upgraded version of the BES detector [13]. A 12-layer vertex chamber (VTC) surrounding the beam pipe provides trigger information. A forty-layer main drift chamber (MDC), located radially outside the VTC, provides trajectory and energy loss (dE/dx) information for charged tracks over 85% of the total solid angle with a momentum resolution of $\sigma_p/p = 0.0178\sqrt{1+p^2}$ (p in GeV/c) and a dE/dx resolution for hadron tracks of $\sim$ 8%. An array of 48 scintillation counters surrounding the MDC measures the time-of-flight (TOF) of charged tracks with a resolution of $\sim$ 200 ps for hadrons. Radially outside the TOF system is a 12 radiation length barrel shower counter (BSC), composed of alternating layers of gas streamer tubes and lead plates. This measures the energies of electrons and photons over $\sim$ 80% of the 4π solid angle with an energy resolution of $\sigma_E/E = 21\%/\sqrt{E}$ (E in GeV). Outside the solenoidal coil, which provides a 0.4 Tesla magnetic field over the tracking volume, is an iron flux return that is instrumented with three double layers of counters that identify muons of momentum greater than 0.5 GeV/c.

A Geant3 based Monte Carlo, SIMBES, which simulates the detector response, including interactions of secondary particles in the detector material, is used in this analysis. Reasonable agreement between data and Monte Carlo simulation is observed in various channels tested, including $e^+e^- \to (\gamma)e^+e^-$, $e^+e^- \to (\gamma)\mu\mu$, $J/\psi \to p\bar{p}$, $J/\psi \to \rho\pi$, and $\psi(2S) \to \pi^+\pi^- J/\psi$, $J/\psi \to l^+l^-$.

Candidate events are required to have the correct number of charged tracks for a given hypothesis. Each track must be well fit to a helix in the polar angle range $|\cos\theta| < 0.84$ and have a transverse momentum above 60 MeV/c. For the decay channels $J/\psi \to \gamma K^+K^-\pi^+\pi^-$, $J/\psi \to \gamma\pi^+\pi^-\pi^+\pi^-$, $J/\psi \to \gamma K^\pm\pi^\mp\pi^+\pi^-$ and $J/\psi \to \gamma p\bar{p}$, at least one photon with energy $E_\gamma > 30$ MeV is required in the barrel shower counter.

TOF and dE/dx information are used for particle identification. For the $K^+K^-\pi^+\pi^-$, $\pi^+\pi^-\pi^+\pi^-$, $K^\pm K^0_S\pi^\mp$, $\phi\phi$, and $p\bar{p}$ channels, two kaons and at least one pion, at least three pions, one kaon and at least two pions, at least one kaon in each ϕ, and both the proton and antiproton must be identified, respectively.

Events are kinematically fitted with four constraints (4C) to the hypotheses: $J/\psi \to \gamma K^+K^-\pi^+\pi^-$, $J/\psi \to \gamma\pi^+\pi^-\pi^+\pi^-$, $J/\psi \to \gamma K^\pm\pi^\mp\pi^+\pi^-$, and $J/\psi \to \gamma p\bar{p}$. A one-constraint (1C) fit is performed for the $J/\psi \to \gamma_{\rm miss} K^+K^-K^+K^-$ hypothesis, where $\gamma_{\rm miss}$ indicates that this photon is not detected. Events with a χ^2 less than 40.0 for a particular channel are selected.

In order to remove backgrounds from non-radiative decay channels, all selected events are subjected to (4C) kinematic fits to the hypotheses:

$$J/\psi \to K^+K^-\pi^+\pi^-, \qquad J/\psi \to \pi^+\pi^-\pi^+\pi^-,$$
$$J/\psi \to K^\pm\pi^\mp\pi^+\pi^-,$$

and are required to satisfy

$$\chi^2(J/\psi \to K^+K^-\pi^+\pi^-) > 20.0$$
$$\quad (\text{for } K^+K^-\pi^+\pi^-),$$
$$\chi^2(J/\psi \to \pi^+\pi^-\pi^+\pi^-) > 10.0$$
$$\quad (\text{for } \pi^+\pi^-\pi^+\pi^-),$$
$$\chi^2(J/\psi \to K^\pm\pi^\mp\pi^+\pi^-) > 10.0$$
$$\quad (\text{for } K^\pm K^0_S\pi^\mp).$$

For the $J/\psi \to \gamma p\bar{p}$ channel, we require that the opening angle of the two charged tracks is smaller than 179°. A detailed Monte Carlo simulation shows that these cuts, referred to below as the J/ψ veto, do not distort the invariant mass distributions around the η_c signal peak.

Two additional variables are used to reject events with wrong final state assignments. The first variable, $|U_{\rm miss}| = |(E_{\rm miss} - |\vec{P}_{\rm miss}|c)|$, is used to reject events with multi-photons and misidentified charged particles. Here, $E_{\rm miss}$ and $\vec{P}_{\rm miss}$ are, respectively, the missing energy and momentum calculated using measured quantities for charged tracks. A second variable, $P^2_{t\gamma} = 4|\vec{P}_{\rm miss}|^2\sin^2(\theta_{t\gamma}/2)$, where $\theta_{t\gamma}$ is the angle between the missing momentum and the photon direction, is used to reduce backgrounds from π^0's. The specific values of the selection requirements for these two kinematic variables are summarized in Table 1.

For the $K^+K^-\pi^+\pi^-$ and $\pi^+\pi^-\pi^+\pi^-$ channels, $|M_{\pi^+\pi^-\pi^0} - M_\omega| > 40$ MeV/c^2 is required to remove

Table 1
Cuts imposed on $|U_{miss}|$ and $P^2_{t\gamma}$ for event selection

Mode ($J/\psi \to \gamma X$)	$\|U_{miss}\|$ (GeV)	$P^2_{t\gamma}$ ($(\mathrm{GeV}/c)^2$)
$\gamma K^+K^-\pi^+\pi^-$	< 0.15	< 0.002
$\gamma\pi^+\pi^-\pi^+\pi^-$	< 0.10	< 0.0015
$\gamma K^\pm K^0_S\pi^\mp$ ($\gamma K^\pm\pi^\mp\pi^+\pi^-$)	–	< 0.003
$\gamma p\bar{p}$	< 0.15	< 0.003

the background from $J/\psi \to \omega\pi^+\pi^-$ and $J/\psi \to \omega K^+K^-$; where a π^0 is associated with the missing momentum. For the $K^+K^-\pi^+\pi^-$ channel, we perform a cut on the K^+K^- invariant mass, $|M_{K^+K^-} - M_\phi| > 20\ \mathrm{MeV}/c^2$, to remove the background due to $\phi(1020)$. For the $\pi^+\pi^-\pi^+\pi^-$ channel, a cut on each $\pi^+\pi^-$ invariant mass, $|M_{\pi^+\pi^-} - M_{K^0_s}| > 25\ \mathrm{MeV}/c^2$, is applied to remove the background from $\gamma K^0_s K^0_s$ events.

For events having more than one photon detected in the shower counter, we use the following cuts to remove possible π^0 background. For the $J/\psi \to \gamma\pi^+\pi^-\pi^+\pi^-$ channel, if there are at least two photons, γ_1 and γ_2, and if $\vec{P}_{miss}$ is in the same plane as the two photons, i.e., $|\hat{P}_{miss} \cdot (\hat{r}_{\gamma 1} \times \hat{r}_{\gamma 2})| < 0.15$, we require that $|M(\gamma_1\gamma_2) - M(\pi^0)| > 60\ \mathrm{MeV}/c^2$. Here $\hat{P}_{miss}$ is the unit vector in the direction of the missing momentum, determined from the charged tracks only; $\hat{r}_{\gamma 1}$ and $\hat{r}_{\gamma 2}$ are unit vectors in the γ_1 and γ_2 directions, determined by the shower counter; and $M(\gamma_1\gamma_2)$ is the invariant mass of the $\gamma_1\gamma_2$ pair, obtained by using $|\vec{P}_{miss}|$ and the angles between $\vec{P}_{miss}$ and the γ_1 and γ_2 directions, where we assume that the missing particle decays to γ_1 and γ_2. The advantage of this technique is that it uses the momenta of charged tracks measured by the MDC, which has good momentum resolution, but does not use the photon energy measurements. For $J/\psi \to \gamma K^+K^-\pi^+\pi^-$, $\gamma K^\pm K^0_S\pi^\mp$, and $\gamma p\bar{p}$, we require that $|M(\gamma_1\gamma_2) - M(\pi^0)| > 50\ \mathrm{MeV}/c^2$ when $|\hat{P}_{miss} \cdot (\hat{r}_{\gamma 1} \times \hat{r}_{\gamma 2})| < 0.14$.

For the $K^\pm K^0_S\pi^\mp$ (with $K^0_S \to \pi^+\pi^-$) channel, the $\pi^+\pi^-$ invariant mass for the K^0_S candidate is required to be within $25\ \mathrm{MeV}/c^2$ of the K^0_S mass. For the $\phi\phi$ (with $\phi \to K^+K^-$) channel, the invariant masses of both candidate ϕ's, corresponding to K^+K^- pairs, are required to be within $20\ \mathrm{MeV}/c^2$ of the ϕ mass.

After event selection, the invariant mass spectra for the individual decay modes are obtained, as shown in Fig. 1. An unbinned maximum likelihood fit using MINUIT [14] is performed to all five channels simultaneously, with the fitting function for a given channel i given by

$$f_i(m) = a_i\big[BW(M, \Gamma, m) \otimes GS(m, \sigma_i)\big]EFF_i(m) + (1 - a_i)BG_i(m),$$

where M and Γ are the mass and width of the η_c, respectively, m is the invariant mass for each event, σ_i is the mass resolution in the η_c region, BW is a Breit–Wigner function describing the η_c signal, EFF_i is an efficiency correction function, and BG_i is a second-order polynomial function describing the background shape. In order to include the experimental resolution, the BW function is folded with a Gaussian resolution function GS with the resolution σ_i fixed at a value determined from the Monte Carlo simulation. The parameters M and Γ and the coefficients of the polynomial function, a_i, are determined from the fit. The log likelihood function for the channel i is given by

$$S_i = -\ln L_i = -\ln\left(\prod_{j=1}^{N_i^{\mathrm{event}}} f_i(m_j)\right),$$

where N_i^{event} is the total number of events. The overall log likelihood function,

$$S = \sum_{i=1}^{5} S_i,$$

is minimized to obtain the fitting results from the five channels simultaneously. The fit result is shown in Fig. 1.

The branching ratio can be calculated using

$$Br = \frac{N_{\mathrm{fit}}/\epsilon}{N_{J/\psi}} = \frac{N}{N_{J/\psi}},$$

where ϵ is the detection efficiency; $N = N_{\mathrm{fit}}/\epsilon$ is the efficiency-corrected number of η_c events obtained directly from the fit and corrected using $Br(K^0_s \to \pi^+\pi^-)$ and $Br(\phi \to K^+K^-)$ [8] where necessary; and $N_{J/\psi} = (57.7 \pm 2.72) \times 10^6$ [15] is the total number of J/ψ events. The numbers of η_c events determined from the fit and the corresponding product branching ratios, by decay channel, are listed in Table 2.

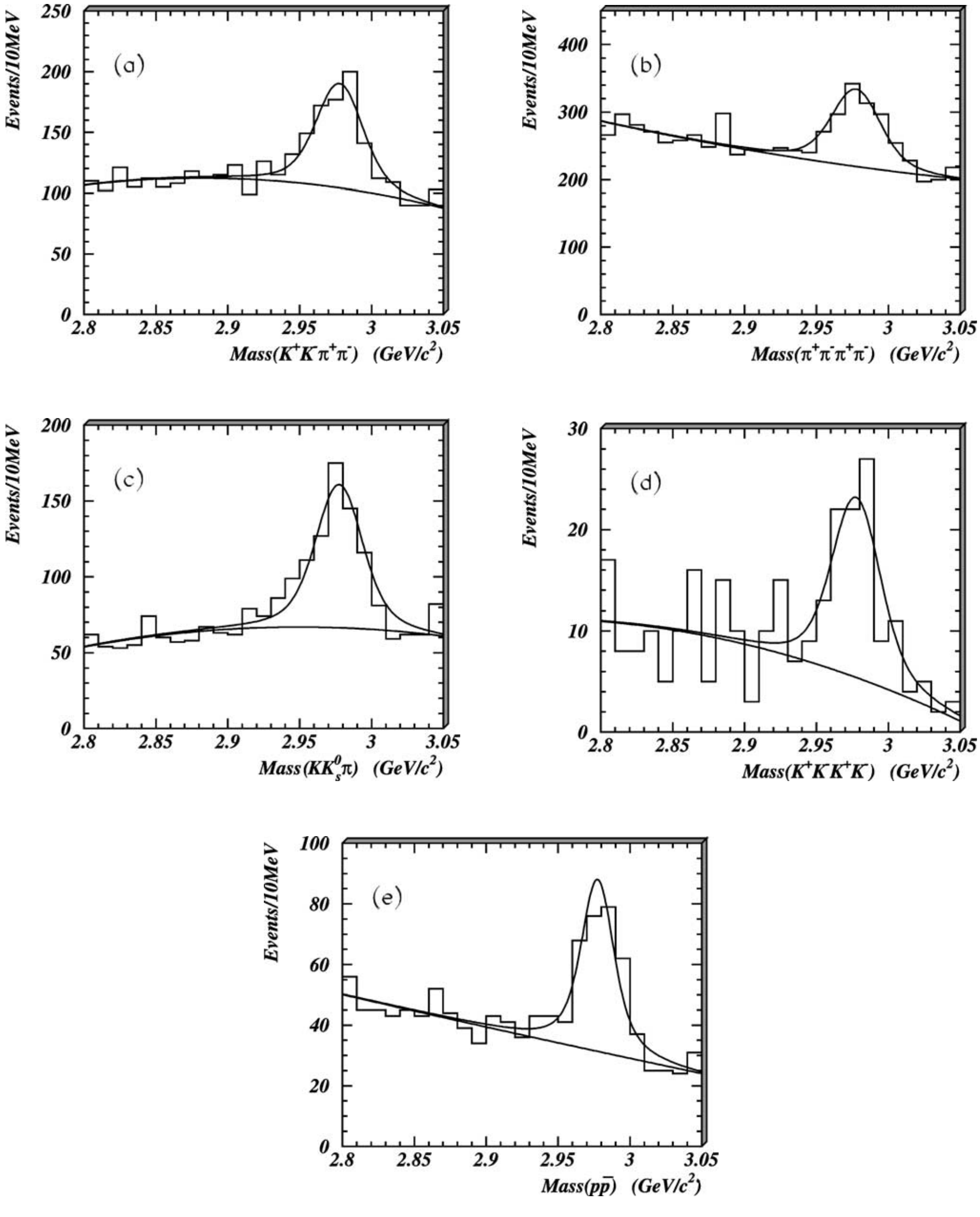

Fig. 1. Invariant mass distributions in the η_c region (a) $m_{K^+K^-\pi^+\pi^-}$, (b) $m_{\pi^+\pi^-\pi^+\pi^-}$, (c) $m_{K^\pm K^0_S\pi^\mp}$, (d) $m_{\phi\phi}$ and (e) $m_{p\bar{p}}$. The histograms correspond to the data; the curves are the fit result.

The main systematic error contributions in measuring the η_c branching ratios originate from uncertainties in the background shape parameterization used, differences between Monte Carlo simulations using different drift chamber wire resolutions, detection efficiency differences due to uncertainties in η_c decay sequences into the final state (for $\eta_c \to \pi^+\pi^-\pi^+\pi^-$, $\eta_c \to K^+K^-\pi^+\pi^-$ and $\eta_c \to K^\pm K^0_S\pi^\mp$), differences in the photon efficiency determined using data and that determined from the Monte Carlo simulation, particle identification uncertainties, and the uncertainty in the total number of J/ψ events. In Fig. 1,

Table 2
Number of η_c events and corresponding branching ratios for the individual channels (corrected using $Br(K_s^0 \to \pi^+\pi^-)$ and $Br(\phi \to K^+K^-)$ [8] where necessary)

Process $J/\psi \to \gamma\eta_c$	No. of events (detected)	No. of events (efficiency-corrected)	Product of branching ratios
$\eta_c \to K^+K^-\pi^+\pi^-$	413 ± 54	8453 ± 1110	$(1.5 \pm 0.2 \pm 0.2) \times 10^{-4}$
$\eta_c \to \pi^+\pi^-\pi^+\pi^-$	542 ± 75	7643 ± 1062	$(1.3 \pm 0.2 \pm 0.4) \times 10^{-4}$
$\eta_c \to K^\pm K_S^0\pi^\mp$	609 ± 71	12516 ± 1460	$(2.2 \pm 0.3 \pm 0.5) \times 10^{-4}$
$\eta_c \to \phi\phi$	357 ± 64	1922 ± 357	$(3.3 \pm 0.6 \pm 0.6) \times 10^{-5}$
$\eta_c \to p\bar{p}$	213 ± 33	1105 ± 171	$(1.9 \pm 0.3 \pm 0.3) \times 10^{-5}$

Table 3
Relative systematic error caused by background shape

Sources	$K^+K^-\pi^+\pi^-$	$\pi^+\pi^-\pi^+\pi^-$	$K^\pm K_S^0\pi^\mp$	$\phi\phi$	$p\bar{p}$
Background polynomial	4.4%	7.6%	2.5%	8.3%	3.2%
Fitting range	9.4%	8.4%	17.2%	15.5%	10.6%
J/ψ veto	1.7%	26.6%	10.1%	17.3%	15.2%

Table 4
Relative systematic error summary

Sources	$K^+K^-\pi^+\pi^-$	$\pi^+\pi^-\pi^+\pi^-$	$K^\pm K_S^0\pi^\mp$	$\phi\phi$	$p\bar{p}$
BG shape	9.4%	26.6%	17.2%	17.3%	15.2%
Wire resolution	10.4%	17.1%	13.1%	2.9%	4.7%
η_c decay sequences	4.5%	4.5%	1.0%	–	–
γ efficiency	2.0%	2.0%	2.0%	2.0%	2.0%
Particle identification	2.5%	2.7%	2.2%	2.5%	1.1%
$N_{J/\psi}$	4.7%	4.7%	4.7%	4.7%	4.7%
Total	15.8%	32.5%	22.3%	18.4%	16.7%

second-order polynomials are used to describe the backgrounds. The systematic errors due to the background shape are studied by using alternative linear polynomial functions to fit the backgrounds in Fig. 1(b), (d), and (e) and third-order polynomials to fit the backgrounds in Fig. 1(a) and (c), changing the upper fitting bound from 3.05 to 3.07 GeV/c^2, and removing the J/ψ veto from the event selection. The relative systematic errors from these sources are listed in Table 3. Since the errors are correlated, we choose the largest one as the systematic error due to the background shape.

The relative systematic errors for the individual channels are summarized in Table 4, where the individual contributions are added in quadrature to obtain the total relative systematic error. The systematic errors on the product branching ratios are given in Table 2.

Using the branching fraction $Br(J/\psi \to \gamma\eta_c) = (1.3 \pm 0.4)\%$ [8], the η_c branching fractions can be obtained. Table 5 shows the BES results together with the PDG [8] and Belle [9,10] values. The BES $Br(\eta_c \to \phi\phi)$ is smaller than the current PDG value of $(7.1 \pm 2.8) \times 10^{-3}$ and is consistent with the Belle [10] and DM2 [3] measurements within errors. The branching fractions for $\eta_c \to K^\pm K_S^0\pi^\mp$ and $\eta_c \to p\bar{p}$ are consistent with both the Belle [9] and PDG values [8]. The branching fractions for $\eta_c \to \pi^+\pi^-\pi^+\pi^-$ and $\eta_c \to K^+K^-\pi^+\pi^-$ are consistent with the PDG values [8] within errors.

Table 5
Branching fractions of the η_c (the Belle results of $Br(\eta_c \to K^{\pm}K_S^0\pi^{\mp})$ and $Br(\eta_c \to p\bar{p})$ are calculated from Ref. [10])

Process	BES (%)	PDG02 (%) [8]	Belle (%)
$Br(\eta_c \to K^+K^-\pi^+\pi^-)$	1.2 ± 0.4	$2.0^{+0.7}_{-0.6}$	–
$Br(\eta_c \to \pi^+\pi^-\pi^+\pi^-)$	1.0 ± 0.5	1.2 ± 0.4	–
$Br(\eta_c \to K^{\pm}K_S^0\pi^{\mp})$	1.7 ± 0.7	$\frac{1}{3}(5.5 \pm 1.7)$	~ 1.8
$Br(\eta_c \to \phi\phi)$	0.25 ± 0.09	0.71 ± 0.28	$0.18^{+0.08}_{-0.06} \pm 0.07$
$Br(\eta_c \to p\bar{p})$	0.15 ± 0.06	0.12 ± 0.04	~ 0.14

Acknowledgements

The BES Collaboration thanks the staff of the BEPC and the IHEP computing center for their efforts. This work is supported in part by the National Natural Science Foundation of China under contracts Nos. 19991480, 10225524, 10225525, the Chinese Academy of Sciences under contract No. KJ 95T-03, the 100 Talents Program of CAS under Contract Nos. U-11, U-24, U-25, and the Knowledge Innovation Project of CAS under Contract Nos. U-602, U-34 (IHEP); by the National Natural Science Foundation of China under Contract No. 10175060 (USTC); and by the Department of Energy under Contract No. DE-FG03-94ER40833 (University of Hawaii).

References

[1] R.M. Baltrusaitis, et al., MARK III Collaboration, Phys. Rev. D 33 (1986) 629.
[2] Z. Bai, et al., MARK III Collaboration, Phys. Rev. Lett. 65 (1990) 1309.
[3] D. Bisello, et al., DM2 Collaboration, Nucl. Phys. B 350 (1991) 1.
[4] R. Partridge, et al., Phys. Rev. Lett. 45 (1980) 1150.
[5] T.M. Himel, et al., Phys. Rev. Lett. 45 (1980) 1146.
[6] C. Baglin, et al., R704 Collaboration, Phys. Lett. B 231 (1989) 557.
[7] H. Albrecht, et al., ARGUS Collaboration, Phys. Lett. B 338 (1994) 390.
[8] Particle Data Group, Phys. Rev. D 66 (2002) 010001-719.
[9] F. Fang, et al., Belle Collaboration, Phys. Rev. Lett. 90 (2003) 071801.
[10] H.-C. Huang, et al., Belle Collaboration, hep-ex/0305068.
[11] J.Z. Bai, et al., BES Collaboration, Phys. Lett. B 555 (2003) 174.
[12] J.Z. Bai, et al., BES Collaboration, Nucl. Instrum. Methods A 458 (2001) 627.
[13] J.Z. Bai, et al., BES Collaboration, Nucl. Instrum. Methods A 344 (1994) 319.
[14] F. James, CERN Program Library Long Writeup D506.
[15] S. Fang, et al., HEP&NP 27 (2003) 277 (in Chinese).